Numerical Study of Advanced Target Design for FIREX-I

H. Nagatomo 1), T. Johzaki 1), H. Sakagami 2) Y. Sentoku 3), A. Sunahara 4), T. Taguchi 5), Y. Nakao 6), H. Shiraga 1), H. Azechi 1), K. Mima 1)

1) Institute of Laser Engineering, Osaka University, Suita, Japan
2) National Institute for Fusion Science, 322-6, Toki, Japan
3) Department of Physics, University of Nevada, Reno, USA
4) Institute for Laser Technology, Suita, Japan
5) Department of Electrical and Electronic Engineering, Setsunan University, Neyagawa, Japan
6) Department of Applied Quantum Physics and Nuclear Engineering, Kyushu University, Fukuoka, Japan

e-mail contact of main author: naga@ile.osaka-u.ac.jp

Abstract. In the fast ignition (FI) scheme, at first high-density fuel core plasma is assembled by implosion laser, and it is then heated by peta watt laser to achieve fusion burning condition. A typical target for FI is a shell fitted with a reentrant Au cone to make a pass for heating laser. It is found that a high-Z material such as Au has disadvantage as a cone material in the long-duration and high-intensity laser case by using one-dimensional (1-D) PIC, and 1-D relativistic Fokker-Planck (FP) simulations. For FIREX-I scale size experiments, CH has advantages in viewpoint of generation of hot electron and the hot electron transport. Implosion is another important process for FI. Following these results of 1-D PIC and 1-D relativistic FP simulations, 2-D non-spherical implosion dynamics with CD tip is investigated. With sophisticated target and laser pulse shape design, CD tip will be realized without breaking up of cone tip before the maximum density timing, and debasement of implosion performance.

1. Introduction

Fast ignition (FI) is an attractive scheme in laser fusion [1,2]. In FI, at first, high-density fuel core plasma is assembled by implosion laser, and then, just around the maximum density time, it is heated by peta watt laser to achieve a fusion burning condition. In the central-hot-spot (CHS) scheme, a highly uniform laser irradiation and strict power balance of a multi-beam laser system are required. On the other hand, such a requirement is relaxed in FI, and the only requirement for the implosion part is to achieve high-density compression. At ILE Osaka University, the first stage of Fast Ignition Realization Experiment (FIREX-I) has started [3]. In the project, high density core plasma which is compressed by GXII will be heated up to 5 keV by Laser for Fast Ignition Experiments (LFEX), ultra-intense short pulse laser [4].

A typical target for FI is a shell fitted with a reentrant cone to make a pass for heating laser. That is, a cone sustains imploding shell target and ablated plasma which has high pressure. Therefore, gold is supposed to be the best material, and less attention is given. Only gold cone target is investigated and designed in most of our works [5,6]. But it should be noted that laser plasma interaction (LPI) which occurs in a cone is very sensitive to cone target material [7]. Also, a tip is irradiated by radiation from imploding shell and ablated corona plasma, and it is blew up by the high pressure of imploded core plasma finally. For a sophisticated target design for sub-ignition experiment, these detail property should be understood. But there are many difficulties for their complicated multi-scale and multi-physics. Therefore, numerical analyses are effective approach for the studies and designs. In this paper, we focus on the cone tip material to improve the heating efficiency with little influence on implosion

dynamics. Also, selection of tip material is important for an implosion dynamics. In this study, we found the possibility to use low-Z material at the tip from viewpoint of implosion dynamics. Dominant plasma parameter in these simulations of implosion and heating processes are quite different, therefore different numerical approaches are required. In section 2, one-dimensional collisional particle-in-cell (PIC) code, and relativistic Fokker-Planck (FP) simulations are performed to optimize the cone tip material. In section 3, two-dimensional radiation hydrodynamics is used for the simulation of cone-guided implosion.

2. Core heating properties of different cone tip materials

In sub-ignition experiments such as the FIREX-I, the compressed core size is so small that the core expansion rapidly proceeds during the external heating by a short pulse laser. For efficient ion heating such a small sized core, the electron-ion relaxation time should be shorter than the time scale of density reduction due to the expansion. The required heating condition for a FIREX-I class CD core is the heating duration of 5 ~ 10 ps and the energy coupling of the 10 kJ heating laser to the core of > 20 % [8]. A cone-guiding scheme providing a high coupling at the previous experiment is hence adopted in FIREX-I. For further enhancement of heating efficiency, the optimization of cone shaping and its positioning were investigated [9, 10]. However, less attention was paid for a cone material. A candidate of the cone material is Au that was used in the previous experiment because of its high solid density and ease in fabrication. In the FIREX-I, the heating laser energy becomes 20 times higher than that in the previous experiments. When the Au cone is irradiated by such an intense laser, the bulk electron temperature in the cone tip becomes very high (a few keV or more), and Au atoms could be ionized to high charge state. It was shown [11-13] that in the longer pulse case compared with the previous experiment, a steepening of the density profile at the laser irradiation surface occurs and it results in lowering the energy coupling of the heating laser to the fast electrons as well as their temperature. Since the ion mobility due to the electric field is proportional to a charge to mass ratio Z/A (Z and A is ionization charge state of ion and its mass number), the rapid steepening occurs in highly ionized case. In addition, the collisional effects (drag and scattering) in the cone become remarkable. The relatively low energy hot electrons (~ 1MeV), which are expected to heat the core mainly, will suffer strong scattering by highly ionized ions, and the hot electrons lose their kinetic energies through the collisional interactions with bulk electrons and resistive fields. Also the return current carried by the bulk electrons will be significantly damped by the increased resistivity. In the present paper, we show the dependence of core heating properties on the cone tip material on the basis of coupled one-dimensional (1-D) simulations; collisional/ionization particle-in-cell (PIC) simulations for intense-laser plasma interactions and Fokker-Planck (FP) simulations for fast electron transport and core heating.

2.1. Generation of hot electrons

In general, the multi-dimensional natures are important in this kind of phenomena. However, full scale multi-dimensional simulations are very expensive. As the first step we focus on one dimensional scenario. 1-D collisional PIC code PICLS1d [14] is used, where the both electrons and ions are mobile. The collisional ionization process based on the Thomas-Fermi model (Equilibrium model) is introduced. We assumed an CH solid target with the density of 1.0 g/cm^3, thickness of 10 μm, and ion and electron temperatures of 100 eV. Pre-plasma of which scale length is 1.0 μm is attached. Figure 1 shows the generated fast electron profiles in the CH target, together with the results in the Au target; (a) temporal profile of beam

intensity, (b) time-integrated spectrum, and (c) angular spreads for each energy components. The beam intensity for the CH target is nearly the same as that for the Au target at the initial phase (t<0.3 ps). At this moment, Te reaches higher than 1 keV and CH ions are fully ionized in the whole solid region. At the later phase, though the beam intensity significantly decreases for the Au target, the beam keeps almost the constant intensity for the CH target. Compared with the Au target, the density steepening proceeds faster in the CH target because of the larger Z/A. However, the resistive damping of return current is much weaker because of low Z, so that the energetic electrons are continuously supplied into the LPI region by the return current even after steepening occurs. In addition, since the number density of bulk electrons in a solid CH region ($n_e \sim 3 \times 10^{23}$cm^{-3} in the fully-ionized case) is smaller by one order of magnitude compared to the highly-ionized solid Au, the electron thermal pressure stays lower than the laser photon pressure even when Te reaches a several keV. Thus, the bulk electrons are continuously pushed by the laser Ponderomotive force and the positive field is generated between the bulk electrons and the remaining ions. This electrostatic field also pulls the electrons into the LPI region. As the result, the fast electrons are efficiently generated even after the density steepening takes place. A comparison of spectrum between the Au and CH cases shows that the shape is similar between two cases, but the number of electrons is larger in the whole energy range for the CH target. The time integrated electron beam energy ($E_{fe} >$ 100 keV) is 15.26 MJ/cm^2 for the CH target and 7.34 MJ/cm^2 for the Au target; the beam energy is about double in the CH target. In addition, for the low-Z CH target case, the angular spread is smaller, especially in low energy region ($E_{fe} < 1$ MeV). These results show that from the view point of fast electron generation, a low-Z CH is favorable as a cone tip material.
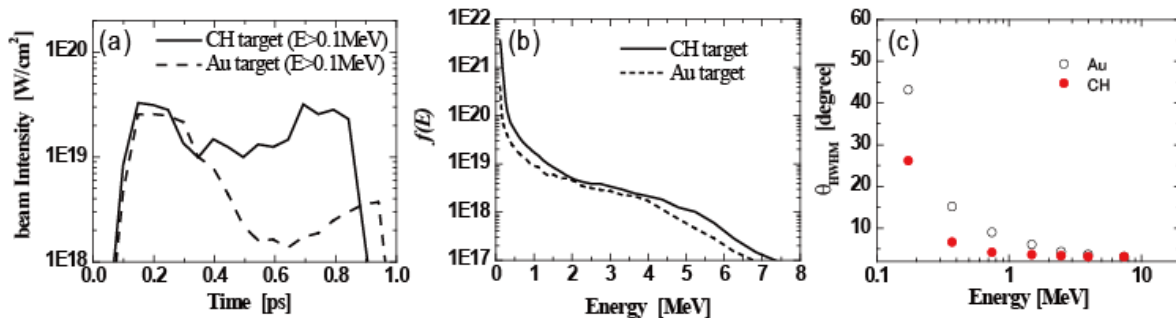

FIG. 1. Comparison of observed fast electron profiles between Au and CH targets. (a) Beam intensity, (b) Energy spectrum, and (c) angular spread (full width at half maximum of angular distribution). In both cases ionization is considered.

2.2. Transport of fast electrons and core heating

Using the fast electron beam observed at the PIC simulation for the CH target, we carried out a 1.2 ps fast electron transport simulation in a solid-density plane CH target with the length of 50 μm and ion and electron temperatures of 100eV. Here, the fast electron transport and core heating processes are simulated using a 1-D relativistic FP –hydro code FIBMET-1D [15] The initial ionization degree is 3.0. In Fig. 2, we showed the injected fast electron profiles and the fast electron profiles observed at x = 5 μm, 10 μm, and 20μm, together with the results for the Au target case. Due to the fast electron beam injection, the electron temperature in the region of x < 30 μm reaches 1keV at t = 0.25 ps and the ions are fully ionized. Compared with the highly-ionized solid Au case, the electron number density in the fully-ionized solid CH target is smaller by one order of magnitude, which means smaller collisional damping. The resistivity ($\propto <Z^2>/T_e^{2/3}$) is also smaller in the CH target for a given electron temperature.

Thus the energy loss of fast electrons during a few tens micron propagation is significantly smaller than that in the Au target, so that the spectrum slightly changes after 20 μm propagation. The current density of fast electron is higher in the CH target, so that the resistive damping becomes relatively larger compared with the collisional damping. In the region within 20 μm, 11.6% of the source energy of fast electron beam is lost. The contributions of the collisional process and the field effect to the energy deposition are 22 % and 78 %, respectively. Compared with a Au target, $<Z^2>$ is significantly lower in a CH target, so that the scattering effect is also weaker in a CH target. The angular spread of fast electron, hence, changes slightly after 20μm propagation for high ($E_{fe} > 2.0$ MeV) and middle (0.3 MeV $< E_{fe} < 2.0$ MeV) energy components though it becomes larger with the propagation length only for the low energy component ($E_{fe} < 0.3$ MeV).
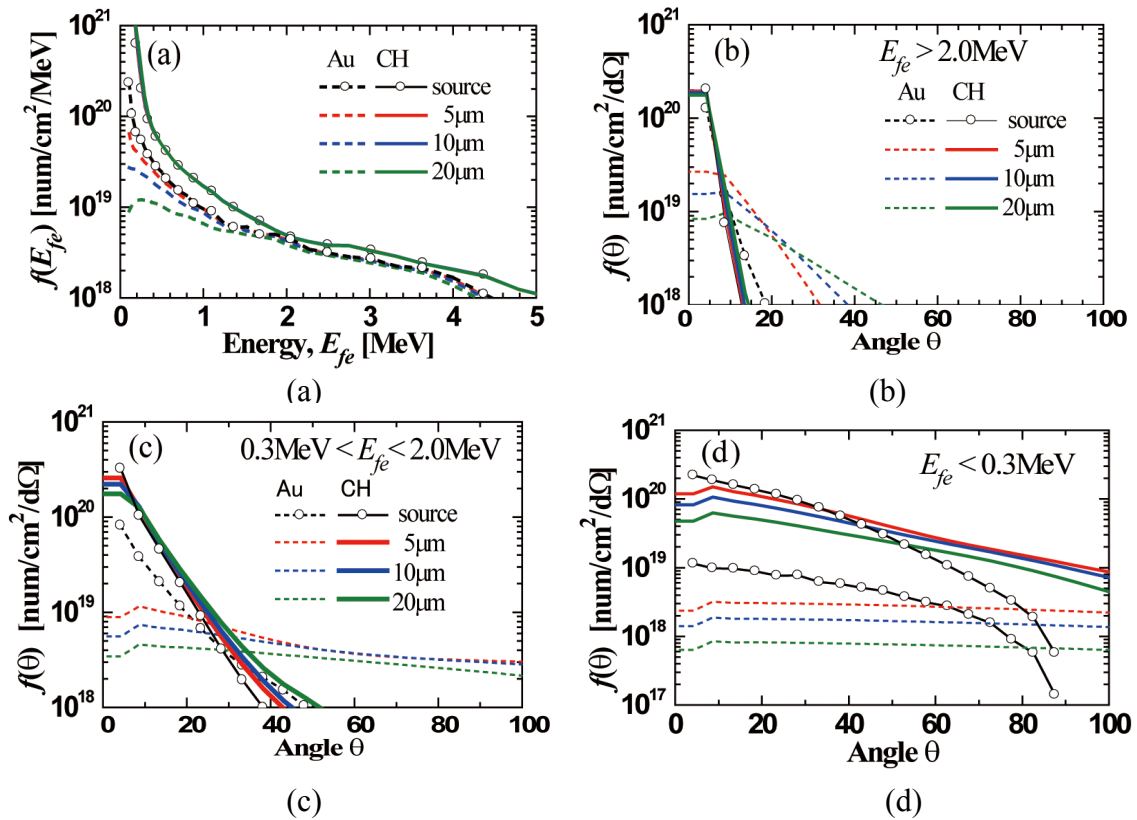

FIG.2. Comparison of generated fast electron profiles between Au and CH targets. (a) Energy spectrum, (b), (c), and (d) angular distributions for high ($E_{fe} > 2.0$ MeV), middle (0.3 MeV $< E_{fe} < 2.0$ MeV) and low ($E_{fe} < 0.3$ MeV) components, respectively. The curves with open circles stand for the source profiles, the colored curves for those observed at x=5 μm (red), 10 μm (blue), and 20 μm (green).

The above results of the generation and transport of fast electrons are taking account into 1-D core heating simulations using FIBMET-1D. A compressed CD core having the Gaussian density profile as FIREX-I experiment scale is assumed. In the result, the energy coupling of the heating laser to the fast electron is twice higher in the CH cone case compared to the Au cone case. The increases in electron and ion temperatures in the core are twice larger in the CH cone case because of larger conversion efficiency from laser to hot electrons.

3. Cone-guided implosion

The heating process follows the implosion process, where fuel core must be highly compressed. A typical target for FI is a shell fitted with a reentrant gold cone to make a pass for heating laser. There are a few significant problems for the cone. At first, the ablated plasma of gold cone interferes with the implosion dynamics, which is quite different from that of conventional CHS approach. Especially, radiation from corona plasma irradiates the gold cone, and the ablated plasma expands into the shell, and reduces the implosion velocity. Recently, we have found the solution to suppress the expansion of the gold cone, which is described in session 3.1. In the conclusion of the previous session, low-Z material, CH is favorable for the tip of the cone from the viewpoint of heating efficiency. But it is difficult for low density material to sustain the high pressure caused by the implosion. Some preliminary simulations were performed to find a possibility of low-Z material at the tip of the cone. Two-dimension radiation hydrodynamic code, PINOCO are applied, in which mass, momentum, electron energy, ion energy, equation of states, laser ray-trace, laser absorption, radiation transport, surface tracing and other related equations are solved simultaneously. Hydrodynamic equations are solved by the Lagragian-based Arbitrary Lagrangian Eulerian (ALE) method, where the ALE-type CIP (Constrained Interpolation Profile) method [16], ALE-CIP is applied. ALE-CIP has enabled the calculation of a large dynamic range such as implosion. Originally, CIP had some characteristics of the Lagrangian method, although the fundamental formulas are done for Eulerian coordinates with high accuracy. This method is also employed to clearly track the interface between the different materials. This tracking system is very useful when multi-material target structures must be considered. The equation of state is based on the quotidian equation of state (QEOS) [17].

3.1. Suppression of expanding Au plasma at outer surface of the cone

In the implosion process, radiation effect from corona plasma is significant. To study this effect, a non-spherical implosion with CH and cryogenic D_2 shell target for FIREX-I experiment is simulated using 2-D radiation hydrodynamics code, PINOCO [6]. A cone with an opening angle of 30 degree is attached to a spherical shell of CH (6 μm thick) and D_2 (10 μm thick). The target is irradiated by uniform laser of which wavelength, energy and pulse duration are λ= 0.53 μm, 3.5 kJ, and 1.5 ns respectively. Figure 3 (a) shows mass density at 1.8 ns in the case without CH coating on the cone. Black lines indicate contact surfaces. Inside the shell, the Au cone is expanding as a result of radiation absorption on the surface. This ablated Au plasma interferes with imploding fuel plasma in the shell. At a contact point between the shell and Au cone, there is a leak of D_2 fuel because radiation heats up the CH shell near the cone, and it is broken at an early time. Because of these defections, the maximum areal density and maximum density reach only 0.097 g/cm^2 and 129 g/cm^3 respectively, which do not fulfill the goal of FIREX-I. To improve the problems, CH coating on the Au cone surface is considered. The thickness of the CH is about 0.5 μm at the tip and linearly increases to 2.5 μm at the contact point with the initial outer shell. Figure 3 (b) shows mass density contours at 1.8 ns in the case with coating on the cone. The gold plasma from the cone is tamped by CH coating, even though gold plasma has a relatively high temperature and starts expanding. The X-ray emitted from the shell is absorbed by the surface of the gold cone because CH coating is opacity thin for the X-rays of which photon energies are between 600eV-1keV. Therefore in the case without CH coating, photon energy density inside the shell is higher than that of the case with CH coating. The maximum areal density and

maximum density are 0.193 g/cm^2 and 176 g/cm^3 respectively (Fig. 4), which are close to the requirement of FIREX-I [2].
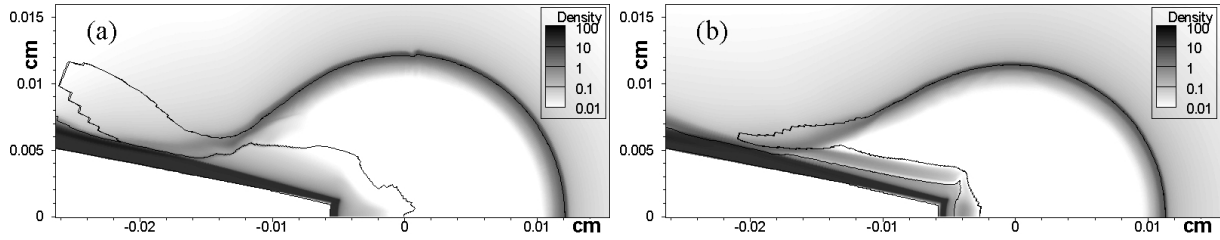

FIG. 3. Mass density contour (g/cm^3) at t=1.8 ns in cone-guided implosion (a) without CH coating and (b) with CH coating respectively.
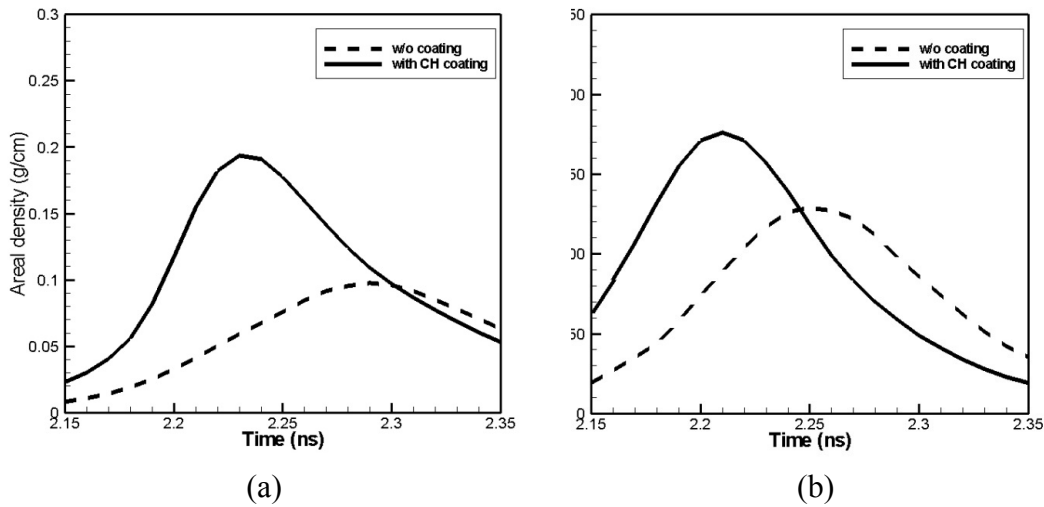

FIG. 4. Time history of (a) areal density, and (b) the maximum density of the case without CH coating (dotted line) and the case with CH coating (solid line), respectively.

3.2. Influence of low-Z tip on implosion dynamics

In section 2, we mention that low-Z material, CH (in this section CH is replaced by CD) is favorable at the tip of the cone from the viewpoint of heating process. But tip is exposed to high pressure plasma at the center of the implosion. Therefore, not only material and shape of the cone, but also implosion dynamics must be designed carefully to reduce damage to tip. In order to investigate the effect of CD tip instead of Au, 2-D radiation hydrodynamics simulations are performed. Figure 5 (a) shows the overview of initial target configuration. The cone with an opening angle of 30 degree is attached to a spherical shell of CD (8 μm thick). The cone has CD layer on both inner and outer surface. The target is irradiated by uniform laser of which wavelength, energy and pulse duration are λ= 0.53 μm, 3.3 kJ, and 1.5 ns respectively. Preliminary, we have simulated the similar condition except a cone, which does not have CD layer on the inner surface. Without this CD layer, radiation from inside the shell is transported into the cone through the CD tip, and absorbed by gold on the inner surface of the cone directly. Due to the radiation heating, inside of the cone is filled with the ablated gold plasma. Same mechanism of CD layer on the Au, which is described in section 3.1 can be applied to the inner surface of the Au cone. For comparison, Au tip (4.5 μm thick with 2 μm CD layer) case is simulated also. Figure 5 (b), and (c) show the mass density contours at maximum compression time in case of Au tip, and CD tip respectively. Both cases

maximum averaged core density and areal density are ρ_{ave}=100 g/cm^3 ρR=0.57 g/cm^2 respectively. Though main part of implosion dynamics are exactly same, tip is deformed easily in case of CD tip.
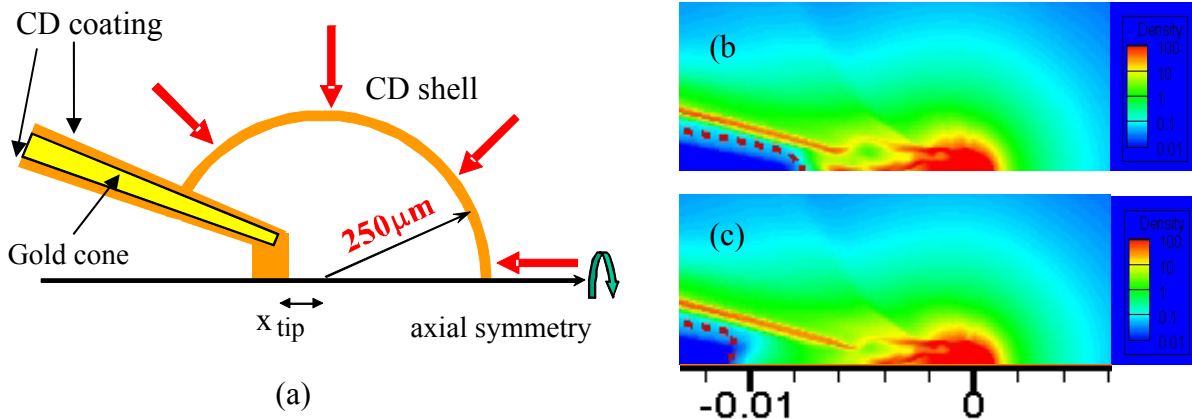

FIG. 5. (a) Configuration of a shell fitted with a reentrant Au cone, which has CD layer inner and outer surface. mass density contours (g/cm^3) at maximum compression time in case of Au tip (a), and CD tip (b) respectively.

To measure property of traveling shockwave inside the cone, another simulation is executed, where a cone is filled with CD solid. Figure 6 shows averaged core density (blue solid line) and positions of shockwave (red square). The first shockwave is leading shockwave of implosion, and the second shockwave is generated by a jet from core. In Fig.5 (b) and (c) at x=-0.04 cm near x-axis, the jets are observed. In non-spherical implosion, there is no laser irradiation at the cone part, and that makes the imbalance of momentum in imploding shell. If a target of CD tip is applied, 40 μm thickness is required. That is, LPI is occurred at 90 μm from center. This distance of 90 μm is unfavorable for fast electron transport, and it should be shorten. Sources of these two shockwaves are controllable. For example, the first shockwave can be weaken if we design a suitable tailored pulse. If spatial distribution of laser intensity is controlled (higher intensity near the cone),the speed of the jet is reduced [18]. This is preliminary study and more realistic simulations is planned.
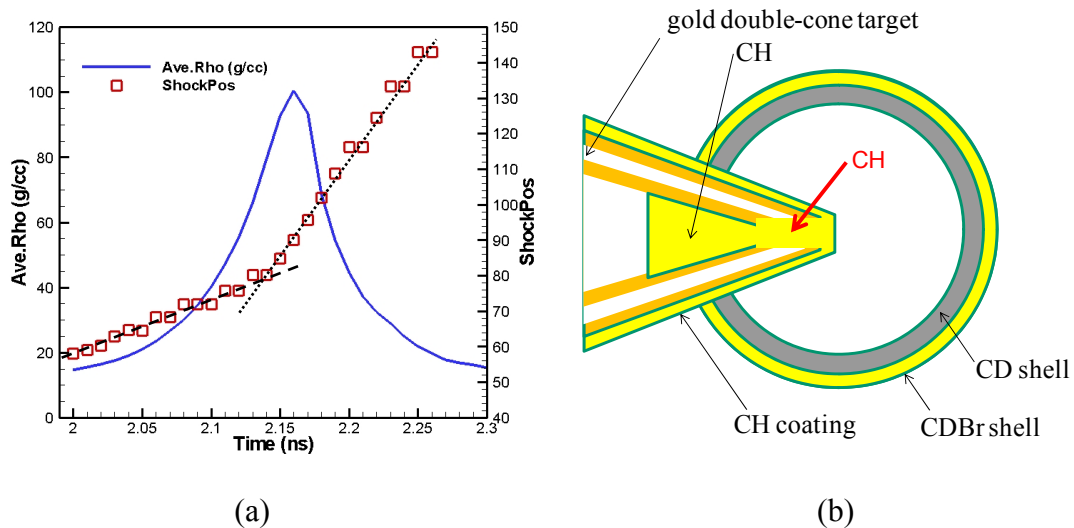

FIG. 6. (a) Averaged core density (blue solid line, g/cm^3), and positions of shockwave (red square). Speed of first shockwave (broken line) is 1.1x10^6 cm/s, and that of second shockwave is 3.1x10^6 cm/s (dotted line). (b) Overview of the advanced target.

Summary

Target designs for FIREX-I, sub-ignition FI experiment is investigated. It is found that a high-Z material such as Au has disadvantage as a cone material in the long-duration and high-intensity laser case. CH is investigated as alternative material for the tip using 1-D PIC and relativistic FP simulations. In result, for FIREX-I scale size LPI, CH has advantages in viewpoint of generation of hot electron and the hot electron transport. Following the proposal of using CH tip, non-spherical implosion dynamics with CD tip is investigated. With sophisticated target and laser pulse shape design, CD tip will be realized without breaking up of cone tip before the maximum density, and debasement of implosion performance. Overview of the advanced target is shown in Fig. 6 (b). Some numerical models are simplified or missing in these studies. For quantitative design, developing some new models, and further detail simulations (multi-dimensional simulations) are necessary.

Acknowledgement

Reference

[1]   TABAK, M., *et. al.*, *Phys. Plasmas* **1**, 1626-1634, (1994).
[2]   KODAMA, R, *et al.* Nature **412** 798 (2001).
[3]   MIMA, K., *et al.*, IAEA-CN-94/IF/03 (2002)
[4]   AZECHI, H., *et al.*, *Plasma Phys. Control. Fusion* **48** B267 (2006).
[5]   H. NAGATOMO, H., *et al.*, IAEA-CN-116/IFP/07-29, (2004).
[6]   H. NAGATOMO, H., *et al.*, *Phys. Plasmas* **14** 056303 (2007).
[7]   JOHZAKI, T., *et al.*, *Plasma Phys. Control. Fusion, to be published.*
[8]   JOHZAKI, T., *et al.*, *Phys. Plasmas, to be published.*
[9]   NAKAMURA T., *et al.*, *Phys. Plasmas* **14** 103105 (2007).
[10] ATZENI, S., *et al.*, *Phys. Plasmas* **15** 056311 (2008).
[11] JOHZAKI, T., *et al.*, *Laser Part. Beams* **25** 621 (2007).
[12] CHRISMAN, B., *et al.*, *Phys. Plasmas* **15** 056309 (2008).
[13] SAKAGAMI, H., *et al.*, *Proceedings of IFSA2007* (2008).
[14] SENTOKU, Y. and KEMP, A. J., *J. Comp. Phys.* **227**, 6846 (2008).
[15] JOHZAKI, *et al.*, *Fusion Sci. Technol.* **43** 428 (2003).
[16] YABE, T., *et al.*, *J. Comp. Phys.* **169**, 556-593 (2001).
[17] MORE, R. M., *et al.*, *Phys. Fluids*, **31**, (10), 3059-3078 (1988).
[18] SHIRAGA, H., , *et al.*, IAEA-CN-165/IF1-2 (2008).